Oncogene (2019) 38:2501–2515
https://doi.org/10.1038/s41388-018-0605-5

ARTICLE

MDM2-mediated degradation of WRN promotes cellular senescence in a p53-independent manner

Boya Liu[1] · Jingjie Yi[2] · Xin Yang[1] · Lu Liu[1] · Xinlin Lou[1] · Zeyuan Zhang[1] · Hao Qi[1] · Zhe Wang[1] · Junhua Zou[1] · Wei-Guo Zhu[3] · Wei Gu[2] · Jianyuan Luo[1]

Received: 19 June 2018 / Revised: 27 September 2018 / Accepted: 13 November 2018 / Published online: 7 December 2018

Abstract

MDM2 (Murine double minute 2) acts as a key repressor for p53-mediated tumor-suppressor functions, which includes cellular senescence. We found that MDM2 can promote cellular senescence by modulating WRN stability. Werner syndrome (WS), caused by mutations of the WRN gene, is an autosomal recessive disease, which is characterized by premature aging. Loss of WRN function induces cellular senescence in human cancer cells. Here, we found that MDM2 acts as an E3 ligase for WRN protein. MDM2 interacts with WRN both in vivo and in vitro. MDM2 induces ubiquitination of WRN and dramatically downregulates the levels of WRN protein in human cells. During DNA damage response, WRN is translocated to the nucleoplasm to facilitate its DNA repair functions; however, it is degraded by the MDM2-mediated ubiquitination pathway. Moreover, the senescent phenotype induced by DNA damage reagents, such as Etoposide, is at least in part mediated by MDM2-dependent WRN degradation as it can be significantly attenuated by ectopic expression of WRN. These results show that MDM2 is critically involved in regulating WRN function via ubiquitin-dependent degradation and reveal an unexpected role of MDM2 in promoting cellular senescence through a p53-independent manner.

Introduction

Werner syndrome (WS) is an autosomal recessive disease characterized by premature aging and cancer predisposition and is caused by mutations of the *WRN* gene [1]. WRN is a member of the RecQ family of DNA helicases, which are conserved from bacteria to humans. All the members possess a core helicase domain. In humans, loss-of-function in other members such as BLM and RecQL4 also lead to genetic diseases: Bloom, and Rothmund-Thomson syndromes, respectively [2]. WRN encodes a multifunctional enzyme consisting of 1432 amino acids that has both ssDNA (single-stranded DNA) -stimulated ATPase with 3′–5′ DNA helicase activity and 3′–5′ exonuclease activity [3, 4]. WRN functions in almost all the process of DNA metabolism, including replication, transcription, recombination, and repair [5]. WRN unwinds a diverse set of DNA structures, such as bubbles, D-loop, Holiday junction, and G-quadruplex [6]. Cells derived from WS patients undergo premature replicative senescence often characterized by defects in telomere maintenance and a prolonged S-phase [7, 8]. Furthermore, WS cells are hypersensitive to various types of DNA damage agents, including 4-nitroquinoline-*N*-oxide, topoisomerase inhibitors, cross-link agents, and other genotoxic agents [7, 9, 10]. Most WRN proteins are localized in nucleoli in normal conditions. However, after DNA damage, it rapidly translocates to the nucleoplasm to form DNA damage foci [11].

WRN can be post-translationally modified by phosphorylation, acetylation, ubiquitination, and sumoylation. It is reported that post-translational modifications (PTMs) regulate many aspects of WRN functionality, including catalytic activities, subcellular localization, and protein partner interactions in response to stress [12]. WRN is

Electronic supplementary material The online version of this article (https://doi.org/10.1038/s41388-018-0605-5) contains supplementary material, which is available to authorized users.

✉ Jianyuan Luo
luojianyuan@bjmu.edu.cn

[1] Department of Medical Genetics, Peking University Health Science Center, 38 Xueyuan Road, 100191 Beijing, China

[2] Institute for Cancer Genetics, Columbia University, New York, NY 10032, USA

[3] Department of Biochemistry and Molecular Biology, Shenzhen University School of Medicine, Shenzhen, China

phosphorylated at serine/threonine and tyrosine by ATM (Ataxia Telangiectasia Mutated), ATR (Ataxia Telangiectasia And Rad3-Related Protein), CDK1 (Cyclin Dependent Kinase 1), DNA-PKcs (DNA-dependent protein kinase, catalytic subunit), and c-Abl (ABL1 Abelson murine leukemia viral oncogene homolog 1) tyrosine kinase [13–17]. Phosphorylation of WRN inhibits WRN exonuclease and helicase activities and is required for its proper accumulation in nuclear foci to prevent breakage of stalled forks following replication stress [14]. It also appears to be essential in the NHEJ (Non-homologous end joining) repair [15]. WRN is acetylated by p300 to facilitate its translocation from the nucleoli to the nucleoplasm, and acetylation both regulates catalytic activities and enhances the role of BER (Base excision repair) [18–20]. WRN is reported to be associated with SUMO-1 (Small Ubiquitin-Like Modifier 1) and Ubc9, but the functional consequence of WRN sumoylation remains elusive [21]. Although WRN degradation by the ubiquitin-mediated proteasome pathway has been reported, the E3 ubiquitin ligase of WRN ubiquitination remains unclear [22–24].

MDM2 is a well-known regulator for suppressing p53. As a RING-type E3 ubiquitin ligase, MDM2 binds to the N-terminus of p53 to promote proteasome-mediated degradation and to interfere with transcriptional activity [25, 26]. MDM2 is also a p53 target gene. Activated p53 simultaneously increases MDM2 transcription in the feedback loop [27]. MDM2 RING finger mutants C462A and Y487A fail to ubiquitinate p53 for degradation [28, 29]. p53 transcriptionally activates genes involved in apoptosis, senescence, and cell cycle arrest [30–32]. In normal cells, MDM2 keeps p53 at very low levels. Upon activation by various genotoxic and cytotoxic stresses, p53 is phosphorylated by DNA-PK at Ser 15, which leads to dissociation with MDM2. Phosphorylation at Ser 15 and 37 impairs MDM2 inhibition of p53-mediated transcription [33]. Besides p53, MDM2 also targets other substrates, such as retinoblastoma (Rb), Phosphoglycerate mutase (PGAM), and Forkhead Box O4 (FOXO4) to regulate their functions [34–36].

In this study, we identified MDM2 as an E3 ligase for the WRN protein. MDM2 interacts with WRN both in vivo and in vitro. MDM2 downregulates the WRN protein by a ubiquitin-mediated proteasome pathway. In Etoposide-treated cells, WRN re-localized to the nucleoplasm and was degraded by the MDM2-mediated ubiquitin–proteasome system upon DNA repair completion, which is p53 independent. The senescent phenotype induced by Etoposide was facilitated by MDM2 and attenuated by ectopic expression of WRN. These results indicate that MDM2 facilitates cellular senescence via ubiquitin-dependent degradation of WRN.

Results

MDM2 interacts with WRN in vivo and in vitro

The interaction between MDM2 and WRN was first assessed with the overexpression system. WRN and MDM2 association was detected in co-transfected 293T cells by reciprocal immunoprecipitations (Figs. 1a, b). To examine the interaction of endogenous WRN and MDM2, HCT116 whole-cell lysates were incubated with control IgG, anti-WRN, or anti-MDM2 antibody, and immunoprecipitates were detected by anti-MDM2 and anti-WRN antibodies. Endogenous MDM2 was co-precipitated with endogenous WRN from HCT116 cell lysates, but not from control IgG (Fig. 1c, upper panel). Conversely, endogenous WRN was also co-precipitated with endogenous MDM2, but not from control IgG (Fig. 1d, upper panel). These results confirm that WRN binds to MDM2 in vivo.

To demonstrate the interaction between WRN and MDM2 in vitro and to determine the specific region of WRN involved in the interaction with MDM2, three truncated WRN GST (glutathione S-transferase) fusion proteins were constructed and subjected to the GST pull-down assay. As shown in Fig. 1e, the C-terminus of WRN (GST-WRN-CT) was found to be sufficient for interaction with MDM2, whereas the N-terminal (GST-WRN-NT) and central domains (GST-WRN-M) showed no binding to MDM2. These data collectively indicate that WRN is physiologically and directly binding to MDM2.

MDM2 regulates WRN stability

When we performed the interaction assay between WRN and MDM2, we noticed that co-transfected MDM2 can downregulate the WRN protein (Fig. 1a, left upper panel, and Fig. 1b, left lower panel). Ectopic MDM2 was able to decrease the level of ectopic WRN in 293T cells in a dose-dependent manner (Fig. 1f). MDM2 is a RING domain dependent E3 ubiquitin ligase that mediates the degradation of p53. When Flag-MDM2 WT or Flag-MDM2 catalytic inactive mutants (MDM2-C462A/MDM2-Y487A) were co-transfected into 293T cells with MYC-WRN, we observed that WRN protein levels were decreased only in the presence of wild-type MDM2 and not in the presence of both catalytic inactive mutants (Fig. 1g). Next, we examined the effect of the proteasome inhibitor MG132 on WRN protein levels. The effect of MDM2 on WRN stability was blocked upon treatment with MG132, indicating that MDM2 promotes WRN degradation through the ubiquitin–proteasome pathway (Fig. 1h).

We performed a cycloheximide (CHX) chase experiment to examine if MDM2 can regulate WRN protein half-life by

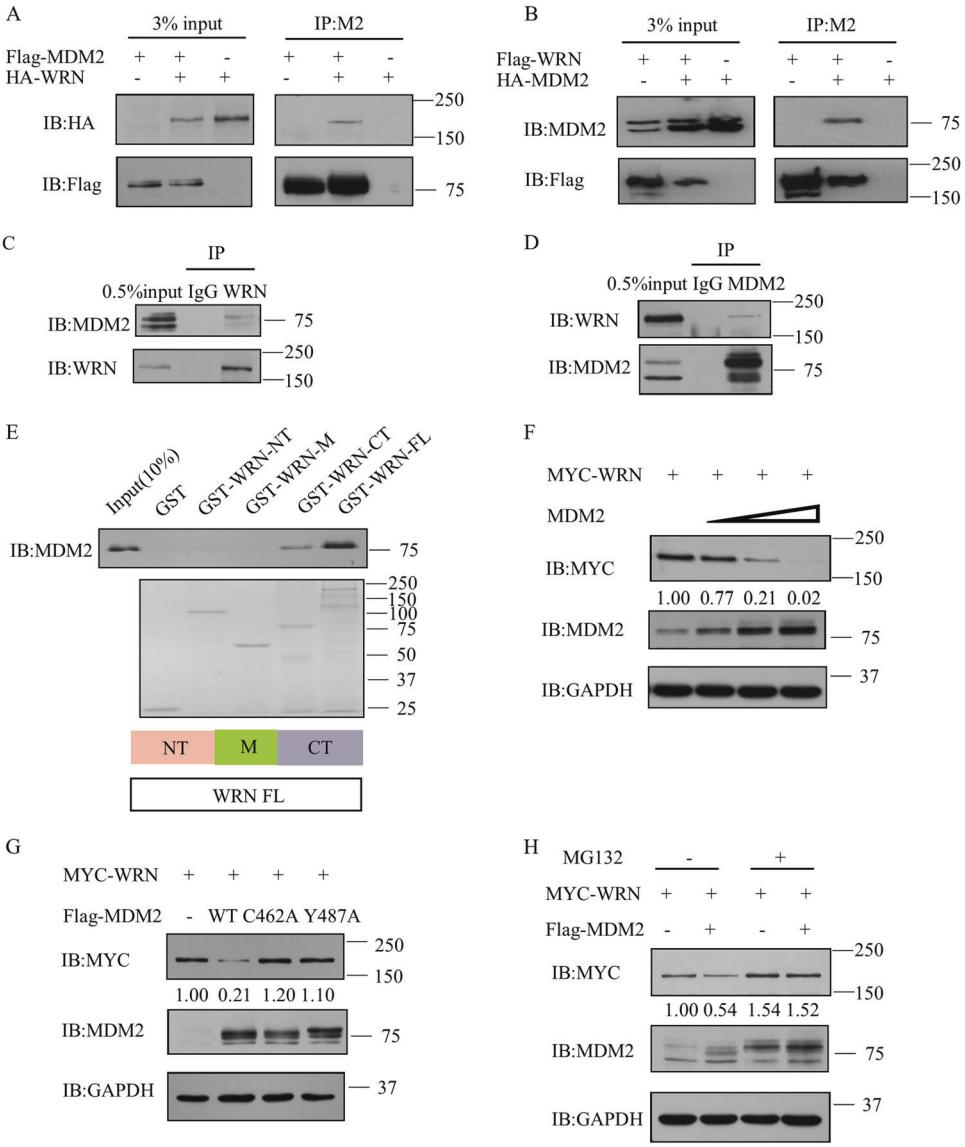

Fig. 1 MDM2 interacts with WRN in vivo and in vitro. **a** Immunoprecipitation analysis for the interaction between Flag-MDM2 and HA-WRN in transfected 293T cells. **b** Co-immunoprecipitation of HA-MDM2 with Flag-WRN. 293T cultures were transfected with the indicated combinations of plasmids producing Flag-WRN and HA-MDM2. **c**, **d** HCT116 cells were treated with 5 μM MG132 for 8 h. The cell lysates were subjected to IP with anti-WRN (H300) or anti-MDM2 (SMP14) and control immunoglobulin. **e** Purified MDM2 was incubated with GST, GST-WRN-CT, GST-WRN-NT, and GST-WRN-M coupled to Glutathione Sepharose resin. The levels of GST fusion proteins are shown in the lower panel. Structure of WRN protein with predicted domains. **f** 293T cultures were transfected with plasmids expressing MYC-WRN (2 μg) and MDM2 (0.5, 1, or 2 μg) as indicated. **g** WRN degradation is dependent on MDM2 E3 ligase catalytic activity. MYC-WRN was ectopically expressed in 293T cells together with wild-type MDM2 and catalytically inactive mutants (MDM2-C462A/MDM2-Y487A). **h** Western blot analysis of WRN level in 293T transfected with indicated constructs and treated MG132

transfecting HCT116 cells with combinations of plasmids producing MYC-WRN and MDM2. When MDM2 was co-expressed, the half-life of WRN decreased dramatically (Fig. 2a). Furthermore, WRN half-life was increased in MDM2 knockout cell lines compared with that in wild-type cell lines (Fig. 2b).

MDM2 facilitates ubiquitination of WRN in vivo and in vitro

As MDM2 destabilized the WRN protein, which was then rescued by MG132, it is likely that MDM2 can ubiquitinate WRN as an E3 ligase. To demonstrate this assumption, we first examined the effect of MDM2 on the ubiquitination of WRN in vivo. Overexpression of MDM2 increased the ubiquitination of WRN in 293T cells (Fig. 2c). To further investigate if MDM2 enhances WRN ubiquitination in a cell-free system, GST-MDM2 was expressed and purified from *Escherichia coli* and Flag-WRN was purified from 293T cells. In vitro ubiquitination assay was performed with Flag-WRN and GST-MDM2, and the results indicate that WRN can be ubiquitinated by MDM2 directly in vitro (Fig. 2d). We further examined MDM2 mutants on WRN ubiquitination, as shown in Fig. 2e; wild-type MDM2 or mutants expression plasmid was co-transfected into 293T cells with His-WRN plasmid. Immunoprecipitated WRN was ubiquitinated in the presence of WT MDM2 but not mutants, which confirms the results indicated in Fig. 1g. As MDM2 knockout is lethal in the presence of p53, we generated MDM2 KO by CRISPR/Cas9 approach in H1299 p53 null cells (Figure S5A–C). MDM2 depletion significantly decreased WRN ubiquitination levels (Fig. 2f).

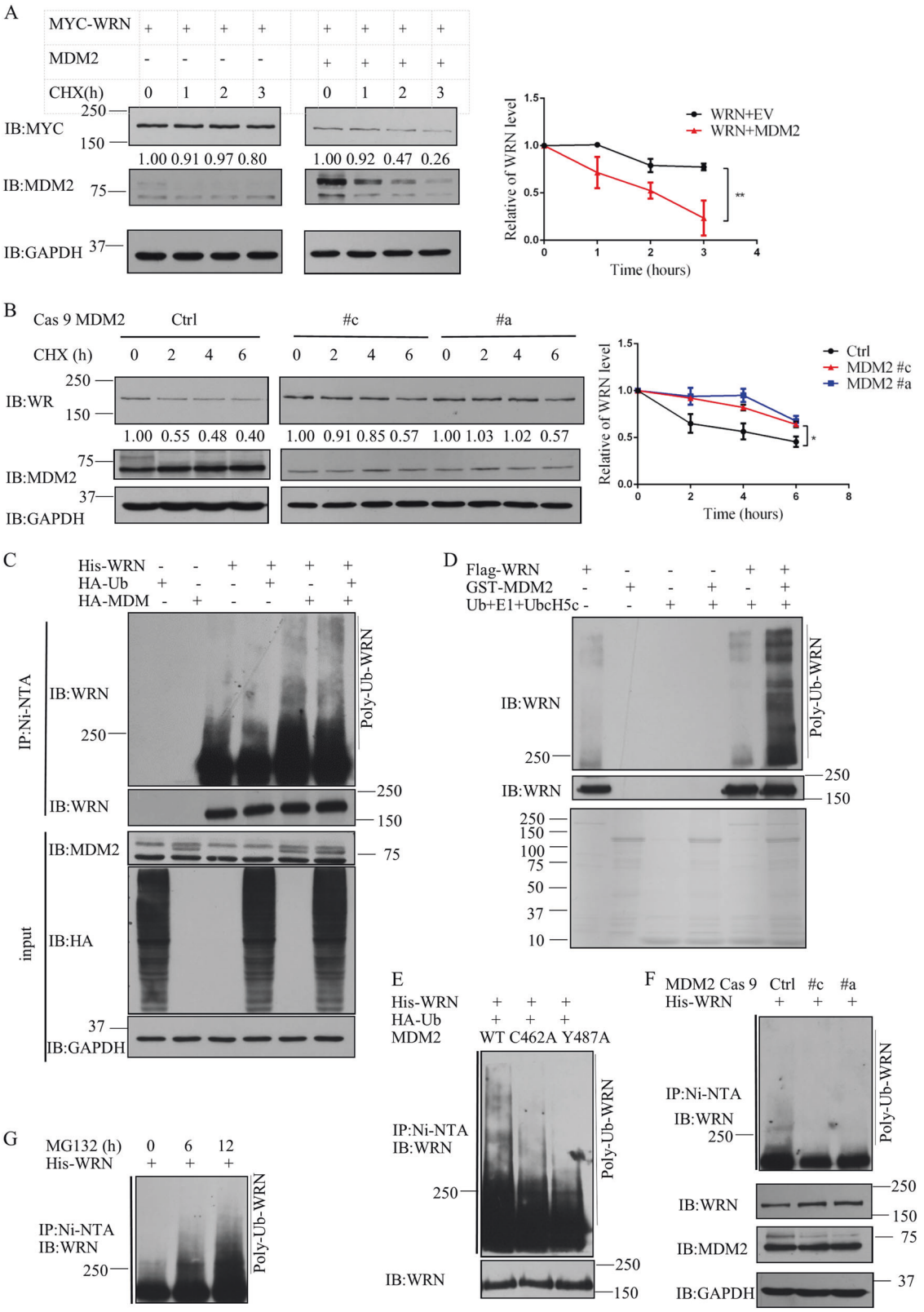

Cells treated with MG132 significantly increased WRN ubiquitination levels (Fig. 2g), indicating that poly-ubiquitination induced WRN degradation through a proteasomal pathway. Together, these data demonstrate that MDM2 is an E3 ubiquitin ligase for WRN both in vivo and in vitro.

◀ **Fig. 2** MDM2 regulates WRN stability and facilitates ubiquitination of WRN. **a** WRN protein stability was examined in the presence of cycloheximide in HCT116 cells transfected with indicated constructs. Shown are representative immunoblots (left) and quantification from two independent experiments (right). One-way ANOVA was used for the statistical analysis. Data are mean ± SEM. *P*-value < 0.01. **b** H1299 cells null of MDM2 were generated using CRISPR-Cas9 genome editing using a MDM2 gRNA designed to target the human MDM2 exon 2. Western blot analysis of WRN level in H1299 generated and treated with cycloheximide. Shown are representative immunoblots (left) and quantification from two independent experiments (right). One-way ANOVA was used for the statistical analysis. Data are mean ± SEM. *P*-value < 0.05. **c** His-WRN expression plasmid was transfected together with or without the plasmid of HA-Ubiquitin (HA-Ub) and MDM2 into 293T cells. WRN protein was enriched under denaturing conditions by using Ni-NTA agarose and immunoblotted by WRN antibody (H300). **d** An in vitro ubiquitination system comprising recombinant UBE1, UbcH5b, GST-MDM2, and ubiquitin was tested for its ability to ubiquitinate full-length Flag-WRN purified from 293T cells. **e** Mutations in MDM2 RING domain impair its ubiquitination activity. 293T cells expressing the indicated forms of MDM2 with His-WRN and HA-Ub plasmids were harvested after 48-h transfection. Immunoprecipitated His-WRN was analyzed by immunoblotting with anti-WRN antibody. **f** MDM2 WT or Cas9 KO H1299 cells were transfected with His-WRN and HA-Ub. Cell lysates were immunoprecipitated using Ni-NTA and then subjected to immunoblotting with anti-WRN antibody. **g** Ubiquitination of overexpressed WRN in HCT116 cells treated with MG132. Cell extracts were immunoprecipitated with Ni-NTA and immunoblotted with WRN antibody

MDM2 regulates WRN stability in response to DNA damage

Under DNA damage conditions, p53 is phosphorylated by ATM on Ser 15, which blocks MDM2-mediated degradation [33]. This raised the question whether freed MDM2 could affect WRN protein by binding to WRN and promoting proteolysis under DNA damage stress. The association of WRN and MDM2 was enhanced upon dose treatment of Etoposide, a topoisomerase II inhibitor, whereas p53 binding to MDM2 was released and stabilized (Fig. 3a). A similar finding was observed in the endogenous situation where more WRN and less p53 were pulled down by MDM2 after Etoposide treatment (Fig. 3b). An immunofluorescence experiment showed WRN translocated from the nucleoli to the nucleoplasm after Etoposide treatment. Colocalization of WRN and MDM2 was detected (Fig. 3c). The same phenomenon was also observed in HCT116 $p53^{-/-}$ cells (Figure S1B).

We examined the stability of WRN protein by blocking protein synthesis with CHX. The half-life of WRN sharply decreased after Etoposide treatment (Fig. 3d). Quantitative real-time PCR analysis revealed that WRN mRNA levels were unchanged after Etoposide treatment (Figure S1A). The examination on WRN ubiquitination found that Etoposide treatment significantly increased WRN ubiquitination levels in cells (Fig. 3e), suggesting that the rapid WRN turnover was due to MDM2-mediated ubiquitination. In line with this data, DNA damage induced WRN ubiquitination was impaired upon MDM2 knockout (Fig. 3f). Further experiments found that WRN protein levels were reduced in both HCT116 WT and p53 null cells after Etoposide treatment, suggesting that DNA damage induced WRN degradation is p53 independent (Fig. 3g). The addition of proteasome inhibitor MG132 restored the WRN protein levels in DNA damage stress cells (Fig. 3h).

MDM2 regulates WRN stability by the MDM2 antagonist Nutlin-3

Nutlin-3 was discovered as a small molecule that binds MDM2 at the p53 interaction site. By disrupting the p53-MDM2 association, Nutlin-3 can lead to improvements in transcriptional activity and p53 stability [37]. Similar to the effect of DNA damage reagent Etoposide, MDM2–WRN association was substantially enhanced by Nutlin-3 treatment, accompanied by a decline in the p53–MDM2 interaction in both overexpression (Fig. 4a) and endogenous conditions (Fig. 4b). To confirm the association, immunofluorescence experiments were carried out in both HCT116 WT and $p53^{-/-}$ cells. As expected, WRN and MDM2 were colocalized upon Nutlin-3 treatment in HCT116 WT cells (Fig. 4c). However, to our surprise, no colocalizations were detected in HCT116 $p53^{-/-}$ cells upon Nutlin-3 treatment (Figure S2B). Half-life experiments show that the WRN protein displayed a faster turnover in cells treated with Nutlin-3 than in untreated cells (Fig. 4d). Quantitative real-time PCR analysis revealed that WRN mRNA levels were unchanged after Nutlin-3 treatment, whereas p53 downstream targets including MDM2 and p21 experienced significantly increased levels (Figure S2A). WRN ubiquitination levels were significantly increased in cells treated with Nutlin-3 (Fig. 4e). WRN ubiquitination was not impaired by Nutlin-3 regardless of whether or not MDM2 was WT or KO in p53 null H1299 cells (Fig. 4f), as Nutlin-3 failed to regulate MDM2 in the absence of p53. Nutlin-3 treatment consistently caused a time-dependent decrease of WRN protein levels in HCT116 p53 WT cells while having no effect on WRN protein levels in HCT116 $p53^{-/-}$ cells (Fig. 4g). Inhibition of the proteasome pathway by MG132 substantially restored WRN protein levels in Nutlin-3-treated cells (Fig. 4h). These results indicate that WRN stability regulated by Nutlin-3 treatment was MDM2 dependent.

MDM2-WRN regulates Etoposide-induced cellular senescence

To investigate the physiological function of MDM2-mediated WRN degradation, we analyzed cell proliferation and cellular senescence after Etoposide treatment. Downregulation of WRN protein contributes to cellular

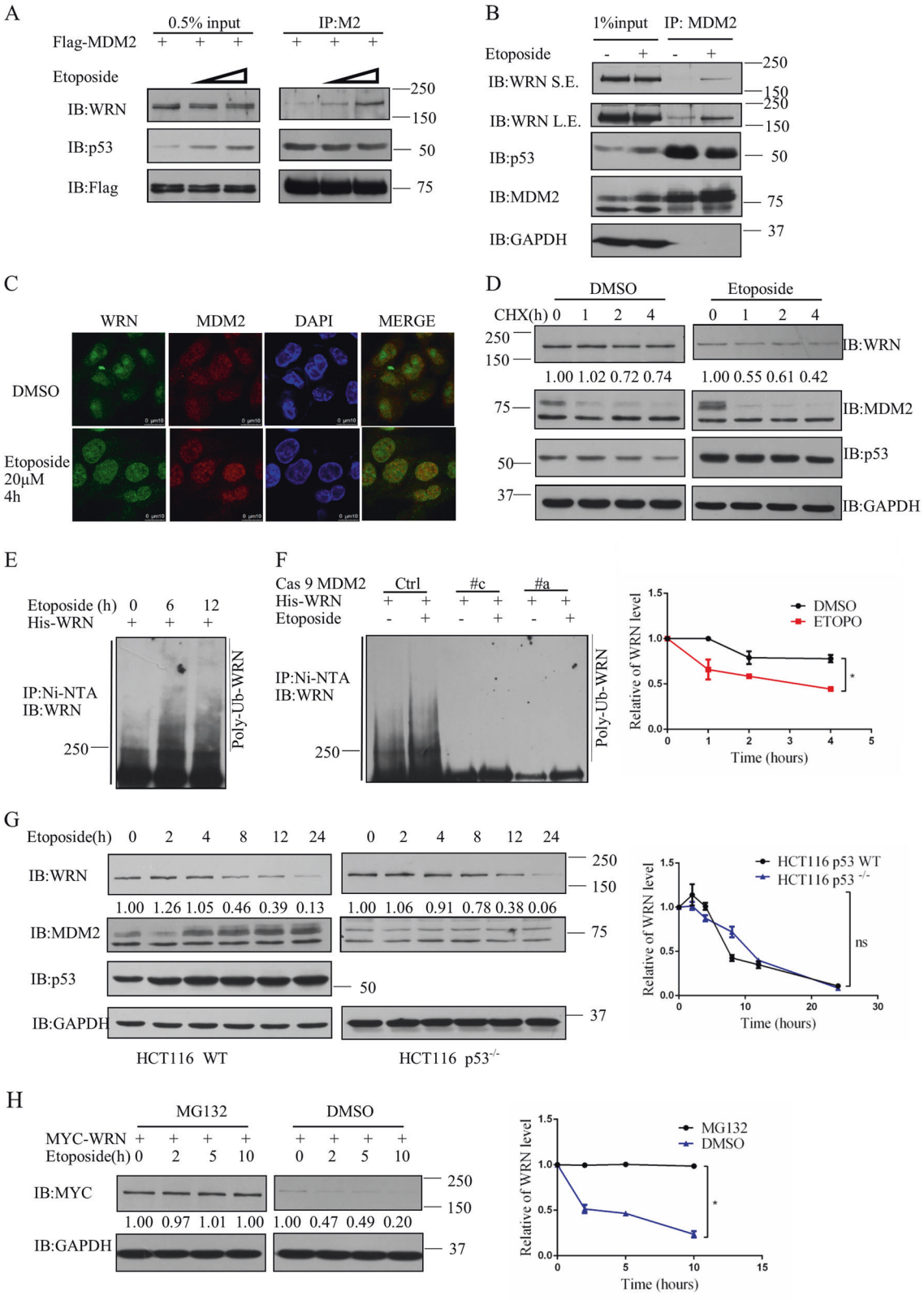

senescence (Figure S5D). Ectopic expression of WRN attenuates the senescent phenotype induced by Etoposide, as shown by senescence-associated β-galactosidase (SA-β-Gal) activity (Fig. 5a) and 5-bromo-2′deoxyuridine (BrdU) incorporation (Fig. 5b) in a dose-dependent manner in HCT116 WT cells. Co-transfection of MDM2 with WRN

◀ **Fig. 3** MDM2 regulates WRN stability in response to DNA damage. **a** DNA damage reagent Etoposide facilitates the physical interaction between WRN and MDM2. 293T cells expressing Flag-MDM2 were treated with 0, 10, 20 μM Etoposide, as indicated. **b** Co-immunoprecipitation of endogenous MDM2 with endogenous WRN and p53. Extracts from HCT116 cells, treated with or without 20 μM Etoposide for 8 h in the presence of 5 μM MG132. **c** Confocal microscopy analysis for the colocalization of WRN and MDM2 in HCT116 p53 WT cells treated with or without 20 μM Etoposide for 4 h. Scale bar as indicated. **d** WRN protein turnover in HCT116 cells treated with or without 20 μM Etoposide. CHX cycloheximide. Shown are representative immunoblots (top) and quantification from two independent experiments (bottom). One-way ANOVA was used for the statistical analysis. Data are mean ± SEM. *P*-value < 0.05. **e** Ubiquitination of overexpressed WRN in HCT116 cells exposed to Etoposide. Cell extracts were immunoprecipitated with Ni-NTA and immunoblotted with WRN antibody. **f** MDM2 restored DNA damage reagent Etoposide-dependent ubiquitination. **g** Immunoblot analysis of whole-cell extracts of HCT116 WT or $p53^{-/-}$ cells incubated with Etoposide (20 μM) for the durations indicated. Shown are representative immunoblots (left) and quantification from two independent experiments (right). One-way ANOVA was used for the statistical analysis. Data are mean ± SEM. The difference is not statistically significant. **h** WRN protein level in HCT116 cells pretreated with MG132 or DMSO for overnight prior to addition of 20 μM Etoposide for the durations indicated. Shown are representative immunoblots (left) and quantification from two independent experiments (right). One-way ANOVA was used for the statistical analysis. Data are mean ± SEM. *P*-value < 0.05

reversed this phenotype (Figs. 5a, b). Compared with control cells, WRN expressed cells showed less signs of senescence including less induction of p53 and p21, whereas co-transfection of MDM2 with WRN reversed the levels of p53 and p21 (Fig. 5c). WRN expressed cells also showed less expression of several SASP genes including IL6, IL8, IL1A, IL1B, CXCL1, and CXCL2 (Fig. 5d). We further examined the protein levels of the two main cytokines known to be associated with senescence, IL6 and IL8, to confirm the results of the mRNA test. By collecting mediums from cultures, we measured the levels of IL6 and IL8 and the results matched the mRNA levels (Fig. 5e). These data indicated that WRN provides protection against Etoposide-induced senescence while overexpression of MDM2 can reverse this effect.

To gain initial insight into how WRN protected cells from senescence induction, we examined whether WRN overexpression alters the recruitment of DNA repair proteins 53BP1 and γH2AX to DSB sites in response to Etoposide treatment. Compared with empty vector, ectopic expression of WRN relatively decreased 53BP1 and γH2AX foci, reduced the levels of DNA damage (Figure S3C). To further understand how MDM2-WRN regulates senescence response, we examined senescence-regulating pathways, p53-p21, p16-Rb and GATA-4-miR-146-NF-κB pathways. We found that cells with WRN overexpression showed less induction of p53 and p21 upon Etoposide treatment (Figure S3D, E), whereas p16-Rb and GATA-4-miR-146-NF-κB pathways are less affected. These data provide an explanation that Etoposide-induced reduction of WRN attenuated DNA damage repair, leading to accumulation of unrepaired DNA and inducing senescence.

MDM2 facilitates cellular senescence is p53 independent

WRN knockdown by RNAi (RNA interference) promotes cellular senescence, which is independent of p53 status (Figure S5D). As WRN protein levels reduced in both HCT116 WT and p53 null cells after Etoposide treatment (Fig. 3g), we explored the protective role of WRN against the cytotoxic effects of Etoposide.

We first investigated whether MDM2-mediated WRN degradation facilitating cellular senescence involves p53, we analyzed cell proliferation and cellular senescence after Etoposide treatment by using HCT116 $p53^{-/-}$ cells. Ectopic expression of MDM2 facilitates the senescent phenotype induced by Etoposide, as shown by SA-β-Gal activity (Fig. 6a) and BrdU incorporation (Fig. 6b) in a dose-dependent manner in HCT116 $p53^{-/-}$ cells. Co-transfection of WRN with MDM2 reversed this phenotype (Figs. 6a, b). Compared with control cells, MDM2 expressed cells showed less WRN protein levels, whereas co-transfection of MDM2 with WRN significantly increased WRN levels (Fig. 6c). WRN expressed cells also showed less expression of several SASP genes including IL6, IL8, IL1A, IL1B, CXCL1, and CXCL2 (Fig. 6d). We further examined the protein levels of the two main cytokines known to be associated with senescence, IL6 and IL8, to confirm the results of the mRNA test. By collecting mediums from cultures, we measured the levels of IL6 and IL8 and the results matched the mRNA levels (Fig. 6e). These results indicated that MDM2 can facilitate cellular senescence in a p53-independent manner and overexpression of WRN can reverse this effect.

DNA damage levels were also examined in HCT116 $p53^{-/-}$ cells. Similar to the results of p53 WT cells, less 53BP1 and γH2AX foci were observed in WRN overexpressed cells upon Etoposide treatment in the absence of p53 (Figure S4C). These results showed that high levels of WRN helped to reduce unrepaired DNA induced by Etoposide, which was p53 independent. We further analyzed p53-p21, p16-Rb, and GATA-4-miR-146-NF-κB pathways. The activated levels of p-p65 and p-Rb rescued by WRN expression in HCT116 $p53^{-/-}$ cells were more pronounced than p53 WT cells (Figure S4D, E). These results showed that WRN played protective role against Etoposide-induced cellular senescence regardless of the presence or absence of p53.

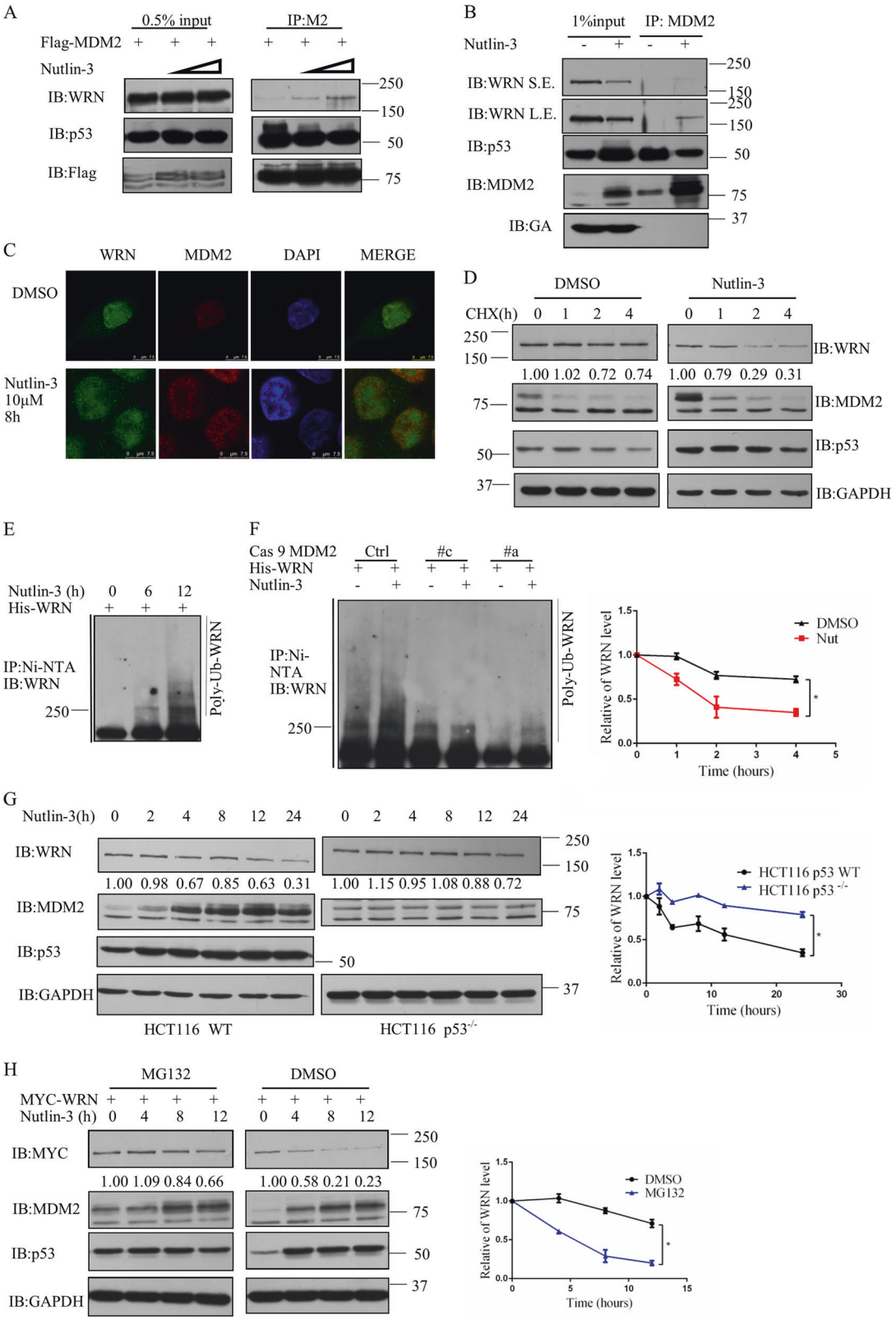
A
0.5% input
IP:M2
Flag-MDM2 + + + + + +
Nutlin-3
IB:WRN
IB:p53
IB:Flag
250
150
50
75
B
1%input
IP: MDM2
Nutlin-3 - + - +
IB:WRN S.E.
IB:WRN L.E.
IB:p53
IB:MDM2
IB:GA
250
150
250
150
50
75
37
C
WRN
MDM2
DAPI
MERGE
DMSO
Nutlin-3
10μM
8h
D
DMSO
Nutlin-3
CHX(h) 0 1 2 4 0 1 2 4
250
150
1.00 1.02 0.72 0.74 1.00 0.79 0.29 0.31
IB:WRN
75
IB:MDM2
50
IB:p53
37
IB:GAPDH
E
Nutlin-3 (h) 0 6 12
His-WRN + + +
IP:Ni-NTA
IB:WRN
250
Poly-Ub-WRN
F
Cas 9 MDM2 Ctrl #c #a
His-WRN + + + + + +
Nutlin-3 - + - + - +
IP:Ni-NTA
IB:WRN
250
Poly-Ub-WRN
Relative of WRN level
DMSO
Nut
Time (hours)
G
Nutlin-3(h) 0 2 4 8 12 24 0 2 4 8 12 24
IB:WRN
250
150
1.00 0.98 0.67 0.85 0.63 0.31 1.00 1.15 0.95 1.08 0.88 0.72
IB:MDM2
75
IB:p53
50
IB:GAPDH
37
HCT116 WT
HCT116 p53-/-
Relative of WRN level
HCT116 p53 WT
HCT116 p53 -/-
Time (hours)
H
MG132
DMSO
MYC-WRN + + + + + + + +
Nutlin-3 (h) 0 4 8 12 0 4 8 12
IB:MYC
250
150
1.00 1.09 0.84 0.66 1.00 0.58 0.21 0.23
IB:MDM2
75
IB:p53
50
IB:GAPDH
37
Relative of WRN level
DMSO
MG132
Time (hours)

◀ **Fig. 4** MDM2 regulates WRN stability by the MDM2 antagonist Nutlin-3. **a** MDM2 antagonist Nutlin-3 facilitates the physical interaction between WRN and MDM2. 293T cells expressing Flag-MDM2 were treated with 0, 5, 10 μM Nutlin-3, as indicated. **b** Co-immunoprecipitation of endogenous MDM2 with endogenous WRN and p53. Extracts from HCT116 cells, treated with or without 10 μM Nutlin-3 in the presence of 5 μM MG132. **c** Confocal microscopy analysis for the colocalization of WRN and MDM2 in HCT116 p53 WT cells treated with or without 10 μM Nutlin-3 for 12 h. Scale bar as indicated. **d** WRN protein turnover in HCT116 cells treated with or without 10 μM Nutlin-3. CHX cycloheximide. Shown are representative immunoblots (top) and quantification from two independent experiments (bottom). One-way ANOVA was used for the statistical analysis. Data are mean ± SEM. *P*-value < 0.05. **e** Ubiquitination of overexpressed WRN in HCT116 cells exposed to Nutlin-3. Cell extracts were immunoprecipitated with Ni-NTA and immunoblotted with WRN antibody. **f** MDM2 restored MDM2 antagonist Nutlin-3-dependent ubiquitination. **g** Immunoblot analysis of whole-cell extracts of HCT116 WT or $p53^{-/-}$ cells incubated with Nutlin-3 (10 μM) for the durations indicated. Shown are representative immunoblots (left) and quantification from two independent experiments (right). One-way ANOVA was used for the statistical analysis. Data are mean ± SEM. *P*-value < 0.05. **h** WRN protein level in HCT116 cells pretreated with MG132 or DMSO for overnight prior to addition of 10 μM Nutlin-3 for the durations indicated. Shown are representative immunoblots (left) and quantification from two independent experiments (right). One-way ANOVA was used for the statistical analysis. Data are mean ± SEM. *P*-value < 0.05

Discussion

WRN regulation through ubiquitination pathways has been reported by our previous study [23] and several other groups [22, 24]. However, the E3 ubiquitin ligase of WRN ubiquitination remains unknown. In this study, we identified MDM2 as the E3 ligase for the WRN protein. MDM2 can directly interact with and regulate WRN protein stability. MDM2 promotes WRN ubiquitination directly with its RING activity. WRN degradation and the senescent phenotype induced by Etoposide was attenuated by ectopic expression of WRN and reversed by MDM2 expression. These results suggest that MDM2 regulates WRN functions via ubiquitin-dependent WRN degradation and this regulation is p53 independent. As MDM2 is the most important p53 regulator, our findings demonstrate a novel p53-independent function for MDM2 beyond the MDM2-p53 regulating axis in response to DNA damage.

Regulation of WRN stability by ubiquitin-dependent degradation has been reported by several groups [22–24]. In response to DNA damage, WRN translocated from the nucleolus to the nucleoplasm for DNA repair. As the WRN protein contains both helicase and exonuclease activities, the excessive WRN proteins in the nucleoplasm may cause unnecessary damage to DNA. Consequently, it is important to keep WRN protein levels low in the nucleoplasm for normal functionality. After DNA repair completion, WRN proteins either translocate back to the nucleoli or degrade. Our findings on WRN degradation by the MDM2-mediated ubiquitin–proteasome system ensures no excessive WRN proteins remain in the nucleoplasm.

WRN ubiquitination is tightly regulated by several factors in response to DNA damage. Our previous study found that p300/CBP mediated acetylation can stabilize the WRN protein by preventing its ubiquitination in response to DNA damage [23]. A recent study by Su and colleagues found that WRN was phosphorylated by ATR at Serine 1141 upon replication stress, and this S1141 phosphorylation led to WRN ubiquitination and degradation [22]. Shamanna and colleagues found that WRN can be ubiquitinated and degraded in Camptothecin-treated breast cancer cells [24]. Our findings on MDM2 as a WRN E3 ligase added a necessary piece to the puzzle.

MDM2 is an E3 ligase for tumor-suppressor p53. It binds to the N-terminus of p53 to promote proteasome-mediated p53 degradation [25, 26]. MDM2 is also a p53 target gene, and activated p53 increases MDM2 transcription in the feedback loop [27]. In normal cells, MDM2 keeps very low levels of p53. In response to various genotoxic and cytotoxic stress, p53 is phosphorylated, leading to disassociation with MDM2 and prevents ubiquitination for stabilization [33]. MDM2 has been found to target other substrates such as Rb, PGAM, and FOXO4 to regulate their functions [34–36]. MDM2 targeting WRN for ubiquitination-mediated degradation links p53 and WRN for synergistic action in response to DNA damage.

The p53 tumor suppressor plays a critical role in inducing cellular senescence [38]. However, besides senescence, p53 can also induce cell growth arrest and apoptosis. How do cells choose to undergo cellular senescence after p53 activation? Previous studies have suggested that the choice of downstream targets, such as p21, plays an important role in determining cell fate [38, 39]. Our studies found that besides p53, MDM2 also specifically ubiquitinated the WRN protein and significantly shortened its half-life. As an E3 ligase for both p53 and WRN, MDM2 could play a critical role in regulating p53 induced cellular senescence. In response to stress, p53 separated from MDM2. As a result, freed MDM2 could interact with WRN protein and ubiquitinate it for its degradation. Cells with activated p53 and lowered WRN proteins could trigger senescence instead of cell growth and apoptosis. Our study increased our understanding of the triggering mechanism for cellular senescence and has the potential to improve the prevention of premature aging.

We found that Etoposide-induced WRN degradation mediated by MDM2 leads to accumulation of unrepaired DNA and facilitate cellular senescence. Overexpression of WRN in Etoposide-treated cells will increase the efficiency of DNA damage response to remove cytotoxic DNA lesions. Generally, two core signal pathways, p16-Rb and p53-p21 pathways, are involved in the process of DNA

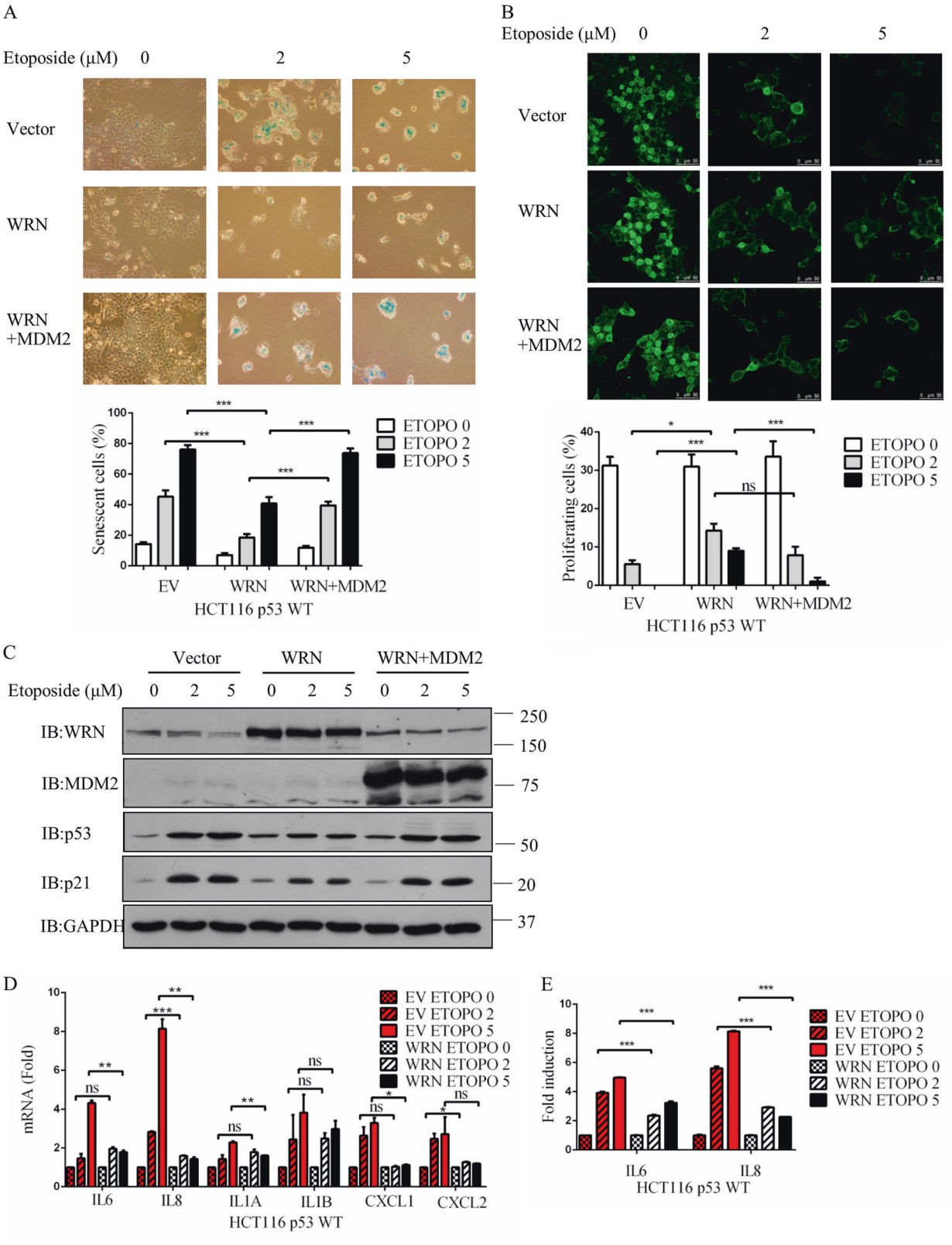

damage-induced senescence. However, recent studies showed that NF-κB pathway also involved in genotoxic agents induced cellular senescence [40, 41]. Our results indicate that p53-p21 pathway played a dominant role in Etoposide-induced senescence in p53 WT cells, however, we could not exclude the role of p16-Rb and NF-κB

◀ **Fig. 5** MDM2-WRN regulates Etoposide-induced cellular senescence. **a** HCT116 p53 WT cells carrying an empty vector or HBLV vector expressing WRN or WRN + MDM2 were grown with indicated Etoposide concentrations for 4 days, and SA-β-Gal staining were analyzed (×200 total magnification). The percentage of cells positive for SA-β-gal in each sample was shown (bottom). At least 300 cells were counted for each sample. Data are mean ± SEM ($N = 3$). *: P-value < 0.05; **: P-value < 0.01; ***: P-value < 0.005. **b** BrdU incorporation of cells from **a** were analyzed. Scale bar as indicated. The percentage of cells positive for BrdU in each sample was shown (bottom). At least 300 cells were counted for each sample. Data are mean ± SEM ($N = 3$). *: P-value < 0.05; **: P-value < 0.01; ***: P-value < 0.005. **c** Cell lysates were subjected to western blot analysis for the indicated proteins. **d** Total mRNA were extracted from HCT116 p53 WT cells expressing WRN or empty vector after 4 days Etoposide induction. Relative mRNA level of IL-6, IL-8, IL-1A, IL-1B, CXCL1, and CXCL2 were determined by quantitative PCR. Data are mean ± SEM ($N = 3$). *: P-value < 0.05; **: P-value < 0.01; ***: P-value < 0.005. **e** Supernatants collected from above cells at day 4 after Etoposide induction were assessed secretory levels of IL-6/8 measured by ELISA. Data are mean ± SEM ($N = 3$). *: P-value < 0.05; **: P-value < 0.01; ***: P-value < 0.005

pathways. In the absence of p53, p16-Rb and NF-κB pathways could be essential for Etoposide-induced senescence. WRN helps to reduce the levels of senescence by decreasing unrepaired DNA induced by Etoposide, whether p53 was proficient or deficient. In both situations, MDM2 acts as an E3 ligase to regulate WRN ubiquitination.

In this study, we found that MDM2 ubiquitinating WRN to facilitate cellular senescence is p53 independent. In cells with wild-type p53, activated p53 with reduced WRN proteins could facilitate cellular senescence instead of cell growth arrest or apoptosis in response to DNA damage. In cells without p53, activating MDM2 could degrade WRN and cause cellular senescence. In this situation, MDM2 could act as a tumor suppressor. This provides a new way to deal with the p53 null tumor and increases our understanding of MDM2 functions.

Materials and methods

Tissue culture and transfection

HEK293T, U2OS, H1299, HCT116 $p53^{+/+}$, HCT116 $p53^{-/-}$ cell lines were maintained in Dulbecco's modified Eagle's medium (Gibco, ThermoFisher, USA) supplemented with 10% fetal bovine serum (Gibco). Transfection of 293T was performed by using the PEI reagent (Polysciences, PA, USA) according to the manufacturer's protocols.

Antibodies

Anti-Flag, MDM2(HDM2-323) antibodies were purchased from Sigma (USA). Anti-HA antibody was from Pierce (ThermoFisher, USA). Anti-WRN (NB100-471) was purchased from Novusbio (CO, USA). The antibodies against p53 (Do-1) (FL-393), p21(C-19), MDM2 (SMP14) (C-18), WRN (H300) (C-19), β-actin were purchased from Santa Cruz Biotechnology (TX, USA). GST resin was from Novagen (Merck, Germany). Anti-Myc and GAPDH were from Cell Signaling Technology (USA). Anti-p16 antibody was purchased from Abcam (USA). Peroxidase-conjugated affinipure Goat anti-mouse IgG (H + L) (Jackson), peroxidase-conjugated affinipure Goat anti-rabbit IgG (H + L) (Jackson, PA, USA), Alexa Fluor 568 donkey anti-mouse IgG (H + L) and Alexa Fluor 488 donkey anti-rabbit IgG (H + L) (Thermo) were used as secondary antibodies.

Co-immunoprecipitation assay

Cells were harvested 48 h after transfection and were lysed in BC100 buffer (100 mM NaCl, 20 mM Tris (pH 7.3), 20% glycerol, 0.2% NP-40). Five percent of the cell lysates was collected as input. Cell extracts were incubated with anti-Flag M2 affinity gel (Sigma) at 4 °C overnight. Beads were washed with BC100 (100 mM NaCl, 20 mM Tris (pH 7.3), 20% glycerol, 0.1% NP-40) for three times and boiled in the sodium dodecyl sulfate (SDS) sample buffer. Protein samples were separated by SDS-polyacrylamide gel electrophoresis (PAGE) and immunoblotted with indicated antibodies.

For endogenous immunoprecipitation, cells were pretreated for 8 with 5 μM MG132 (Sigma) before harvest, then lysed with BC100 buffer (100 mM NaCl, 20 mM Tris (pH 7.3), 20% glycerol, 0.2% NP-40). Five percent of the cell lysates was collected as input. Cell extracts were incubated with 1 μg anti-WRN (H300), anti-MDM2 (SMP14) or normal rabbit IgG, normal mouse IgG (Santa Cruz Biotechnology) at 4 °C overnight. Protein A/G agarose beads (Santa Cruz Biotechnology) were added to the lysates and incubated for 6 h at 4 °C. Agarose beads were washed three times with BC100 buffer and boiled in the SDS sample buffer. Protein samples were separated by SDS-PAGE and immunoblotted with indicated antibodies.

Protein purification

GST and GST fusion proteins were expressed in Rosetta (DE3) (Transgen, Beijing, China) bacterial cells, treated with 0.8 M IPTG (Sigma) to induce fusion protein expression. After 16 h, bacterial cells were harvested and resuspended in phosphate-buffered saline (PBS), then added same volume of BC1000 (1 M NaCl, 20 mM Tris (pH 7.3), 40% glycerol, 2% Triton X-100) to lysed by sonication and purified using the GST-agarose column.

Flag-WRN or MDM2 were purified from 293T cells. After 48-h transfection, cells were harvested and suspended

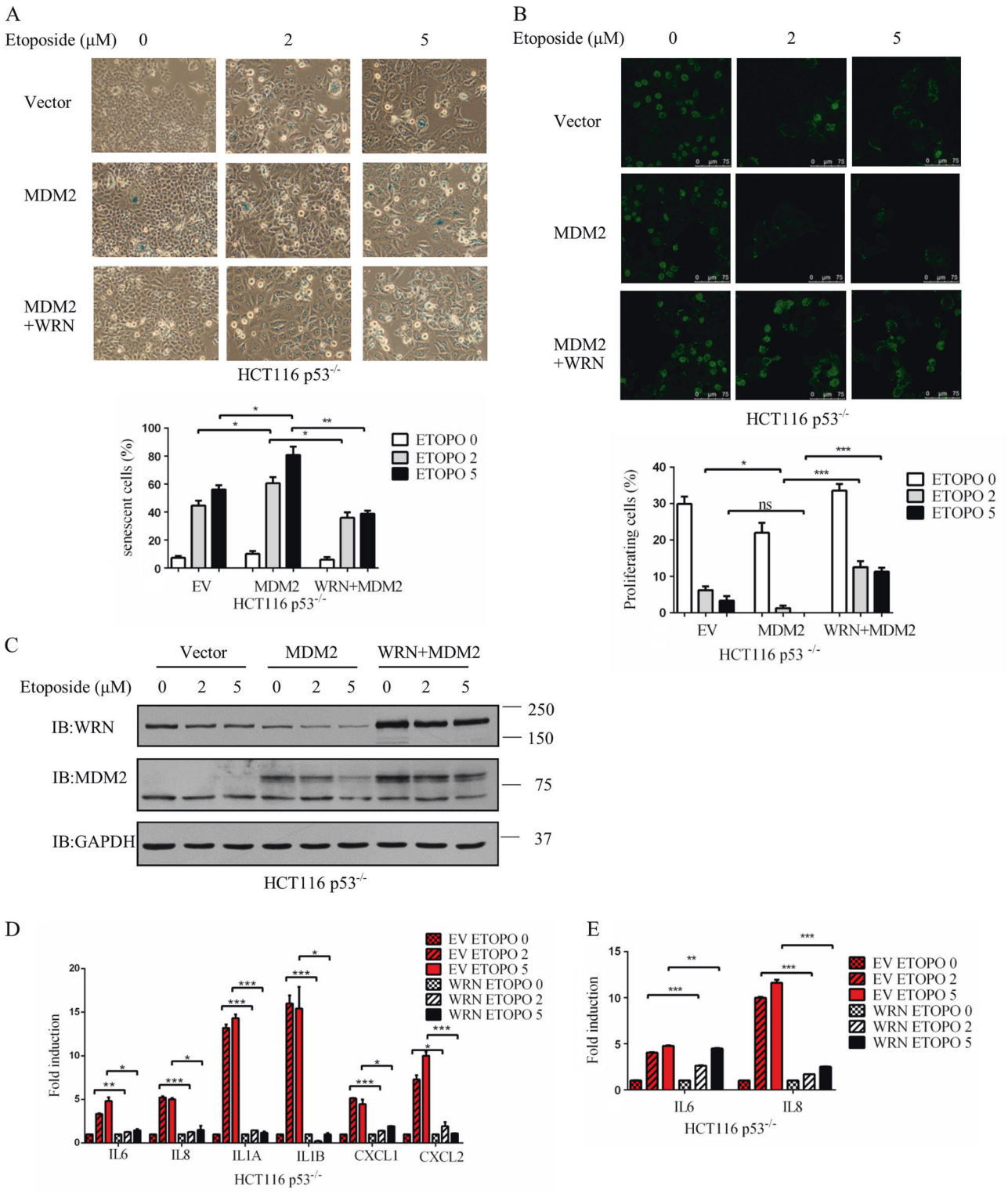

in PBS, then lysed by sonication and added with same volume of BC1000. Cell extracts were incubated with anti-Flag M2 beads at 4 °C overnight. The beads were washed with BC100 for three times then eluted with Flag peptide (Sigma).

GST pull-down assay

Flag-tagged MDM2 or WRN was purified from 293T cells. GST and GST fusion proteins were purified from Rosetta (DE3) bacterial cells and bound to GST-agarose column. In

◀ **Fig. 6** MDM2 facilitates cellular senescence is p53 independent. **a** HCT116 $p53^{-/-}$ cells carrying an empty vector or HBLV vector expressing MDM2 or WRN + MDM2 were grown with indicated Etoposide concentrations for 4 days, and SA-β-Gal staining were analyzed (×200 total magnification). The percentage of cells positive for SA-β-gal in each sample was shown (bottom). At least 300 cells were counted for each sample. Data are mean ± SEM ($N = 3$). *: P-value < 0.05; **: P-value< 0.01; ***: P-value < 0.005. **b** BrdU incorporation of cells from **a** were analyzed. Scale bar as indicated. The percentage of cells positive for BrdU in each sample was shown. At least 300 cells were counted for each sample (bottom). Data are mean ± SEM ($N = 3$). *: P-value < 0.05; **: P-value < 0.01; ***: P-value < 0.005. **c** Cell lysates were subjected to western blot analysis for the indicated proteins. **d** Total mRNA were extracted from HCT116 $p53^{-/-}$ cells expressing WRN or empty vector after 4 days Etoposide induction. Relative mRNA level of IL-6, IL-8, IL-1A, IL-1B, CXCL1, and CXCL2 were determined by quantitative PCR. Data are mean ± SEM ($N = 3$). *: P-value < 0.05; **: P-value < 0.01; ***: P-value < 0.005. **e** Supernatants collected from above cells at day 4 after Etoposide induction were assessed secretory levels of IL-6/8 measured by ELISA. Data are mean ± SEM ($N = 3$). *: P-value < 0.05; **: P-value < 0.01; ***: P-value < 0.005

all, 1 μg Flag-MDM2 or WRN and 10 μg GST fusion proteins were incubated at 4 °C overnight in buffer BC200 (200 mM NaCl, 20 mM Tris (pH 7.3), 20% glycerol, 0.1% NP-40). Beads were washed with BC100 (100 mM NaCl, 20 mM Tris (pH 7.3), 20% glycerol, 0.1% NP-40) for three times and boiled in the SDS sample buffer. Protein samples were separated by SDS-PAGE and immunoblotted with indicated antibodies.

Protein half-life analysis

Cells were pretreated with dimethylsulfoxide (DMSO) or Etoposide (20 μM) (Selleckchem, USA)/Nutlin-3 (10 μM) (Selleckchem) for 8 h, followed by the addition of 100 μg/ml CHX (Selleckchem) into the culture medium. At various time points, cells were collected and subjected to immunoblot analysis.

Plasmids

Flag-, Myc-His-, HA-tagged WRN were cloned into pcDNA3.1 vector. Flag-, HA-tagged MDM2 were cloned into pcDNA3.1 vector. GST-tagged WRN and WRN mutants were cloned into pGEX-4T-3 vector. WRN full length was cloned into pHBLV vector.

In vivo ubiquitination assay

293T cells cultured in 100 mm dishes were transfected with 5 μg His-WRN and/or 5 μg HA-Ub and/or 5 μg MDM2. After 48 h, cells were harvested and resuspended in PBS. Five percent of the cell suspension was collected as input. The remain cells were lysed in buffer PI (6 M guanidine-HCl, 20 mM imidazole, 0.2% Triton X-100, 10 mM β-Me, 500 mM NaCl, 20 mM Na_2HPO_4/NaH_2PO_4, 10 mM Tris (pH 8.0)), then sonicated for 15 pulses. Whole-cell lysates were mixed with Ni-NTA agarose beads (Qiagen, USA) at 4 °C overnight. Ni-NTA beads were washed once with buffer PI, once with buffer PII (8 M urea, 20 mM imidazole, 0.1% Triton X-100, 10 mM β-Me, 500 mM NaCl, 0.1 M Na_2HPO_4/NaH_2PO_4, 10 mM Tris (pH 8.0)), and three times with PIII (8 M urea, 20 mM imidazole, 0.2% Triton X-100, 10 mM β-Me, 500 mM NaCl, 20 mM Na_2HPO_4/NaH_2PO_4, 10 mM Tris (pH 6.3)). Bound proteins were eluted by Elution buffer D (200 mM imidazole, 30% glycerol, 0.72 M β-Me, 0.15 M Tris (pH 6.7)) than neutralized with 1 M Tris and subjected to immunoblot analysis with 59:1 acrylamide: Bis SDS-PAGE.

In vitro ubiquitination assay

Flag-WRN was purified from 293T cells. GST, GST-MDM2, and GST mutants was purified from Rosetta (DE3) bacterial cells. UBE1 (E-305), UBCH5b (E2-627), ubiquitin (U-100H), and ERS (B-10) were purchased from Boston Biochem. Components were mixed to final concentration of 200 μM UBE1, 1 μM UBCH5b, 0.5 mM ubiquitin in ubiquitination assay buffer (20 mM DTT, 500 mM Tris (pH 7.4), 50 mM $MgCl_2$). After preincubation for 10 min at 37 °C with 5 μM Ubiquitin Aldehyde (Santa Cruz), reactions were started by adding ERS (containing ATP). After incubation at 37 °C for 2 h, reactions were ended with SDS loading buffer. Samples were separated by SDS-PAGE followed by Gelcode blue stain reagent (Thermo) staining or immunoblot analysis.

RT-qPCR: RNA extraction, cDNA synthesis and PCR

Total RNA was extracted using Trizol reagent (Sigma) according to manufacturer's protocol, and reverse-transcribed into first-strand complementary DNA (cDNA) using Revertra ace qPCR RT kit (TOYOBO, USA) with random primer. Real-time PCR was performed in triplicate using AceQ qPCR SYBR green master mix (Vazyme, Nanjing, China) by the ABI 7500/7500 fast Real-Time PCR systems (Applied Biosystems, ThermoFisher, USA). The human ACTB was used as internal controls. The following primers were used:

p21 (CDKN1A)	Forward	CTGTCACTGTCTTGTACCCTTGT
	Reverse	GGTAGAAATCTGTCATGCTGGT
actin (ACTB)	Forward	GGACTTCGAGCAAGAGATGG
	Reverse	AGGAAGGAAGGCTGGAAGAG
IL-6	Forward	TGAAAGCAGCAAAGAGGCACTG

Table (continued)

	Reverse	TGAATCCAGATTGGAAGCATCC
IL-8	Forward	AAGGAAAACTGGGTGCAGAG
	Reverse	ATTGCATCTGGCAACCCTAC
WRN	Forward	TGCTAGTGATTGCTCTTTCCTG
	Reverse	CTTTGCCAAGTTTCCCTCTATTG
TP53	Forward	GCCATCTACAAGCAGTCACA
	Reverse	TCATCCAAATACTCCACACGC
MDM2	Forward	TGC CAA GCT TCT CTG TGA A
	Reverse	CGA TGA TTC CTG CTG ATT GA
IL-1A	Forward	GGTTGAGTTTAAGCCAATCCA
	Reverse	TGCTGACCTAGGCTTGATGA
IL-1B	Forward	CTGTCCTGCGTGTTGAAAGA
	Reverse	TTGGGTAATTTTTGGGATCTACA
CXCL1	Forward	GCTGAACAGTGACAAATCCAAC
	Reverse	CTTCAGGAACAGCCACCAGT
CXCL2	Forward	CCCATGGTTAAGAAAATCATCG
	Reverse	CTTCAGGAACAGCCACCAAT

Lentiviral production and infection

Lentiviruses were produced by co-transfecting pHBLV plasmid containing WRN or Lenti-CRISPR-V2 plasmids containing gRNA, and helper virus packaging plasmids pSPAX2 and pMD.2G (at 4:3:1 ratio) into 293T cells. Viruses were harvested at 48 h post-transfection. Following infection, cells were selected for stable expression of the using 1 μg/ml puromycin.

SA-β-gal activity

SA-β-gal activity was detected in cells treated with Etoposide or Nutlin-3 for 4 days using the senescence β-galactosidase staining kit (Cell Signaling Technology), according to the manufacturer's protocol. SA-β-gal+ cells were quantified as percentage of the total number of cell analyzed.

Proliferation assay

Cells were labeled with BrdU (10 μM, Sigma) for 4 h. BrdU-labeled cells were detected by immunostaining using mouse anti- BrdU antibody (1:100, BD Science, USA) and donkey anti-mouse IgG (H + L), FITC (Fluorescein isothiocyanate)-conjugated secondary antibody (Thermo). Antibody binding was visualized by confocal. BrdU-positive cells were quantified as percentage of the total number of cell analyzed.

Immunofluorescence assay

Cells were cultured onto coverslip treated with DMSO or Etoposide or Nutlin-3. To detect WRN and MDM2, we performed fixation with 4% PFA (paraformaldehyde) for 20 min, permeabilization in 0.3% Trition X-100 for 20 min and blocking in goat serum for 2 h. Cells were incubated with specific primary antibody: rabbit WRN antibody (H300), mouse MDM2 antibody (SMP14) for 4 °C overnight diluted in bovine serum albumin (BSA), followed by species specific fluorescein-conjugated secondary antibodies (Alexa Fluor 568 donkey anti-mouse IgG (H + L) or Alexa Fluor 488 donkey anti-rabbit IgG (H + L)) and counterstained with DAPI (4′,6-diamidino-2-phenylindole). Slides were analyzed with Leica TCS-SP8 STED 3 ×.

ELISA

IL-6/8 were detected in cells treated with Etoposide or Nutlin-3 for 4 days using the IL-6/8 human uncoated ELISA kit (Invitrogen, ThermoFisher, USA), according to the manufacturer's protocol.

Statistical analysis

Statistical significance was calculated by Student's *t*-test if no special instructions. Graph-Pad Prism 6 software was used to generate graphs and analyses. Two-sided *P*- values are presented. *: *P*-value < 0.05; **: *P*-value < 0.01; ***: *P*-value < 0.005.

Acknowledgements We thank Dr. Jiadong Wang for generously providing Lenti-CRISPR-V2 plasmid. HCT116 $p53^{-/-}$ cell is a kind gift from Dr. Xiaojuan Du.

Author contributions BL and JL designed research; BL, JY, XY, LL, XL, ZZ and JZ performed research; BL, ZW, HQ, W-GZ and JL analyzed data; and BL, WG, and JL wrote the paper.

Funding This work was supported by National Natural Science Foundation of China (81270427, 81471405, 81671389, 81720108027 and 81321003) and from National Research Program of National Natural Science Foundation of China China (973 Program, 2013CB530801).

Compliance with ethical standards

Conflict of interest The authors declare that they have no conflict of interest.

References

1. Muftuoglu M, Oshima J, von Kobbe C, Cheng WH, Leistritz DF, Bohr VA. The clinical characteristics of Werner syndrome: molecular and biochemical diagnosis. Hum Genet. 2008; 124:369–77.

2. Bernstein KA, Gangloff S, Rothstein R. The RecQ DNA helicases in DNA repair. Annu Rev Genet. 2010;44:393–417.
3. Bohr VA, Cooper M, Orren D, Machwe A, Piotrowski J, Sommers J, et al. Werner syndrome protein: biochemical properties and functional interactions. Exp Gerontol. 2000;35:695–702.
4. Huang S, Li B, Gray MD, Oshima J, Mian IS, Campisi J. The premature ageing syndrome protein, WRN, is a 3'-->5' exonuclease. Nat Genet. 1998;20:114–6.
5. Croteau DL, Popuri V, Opresko PL, Bohr VA. Human RecQ helicases in DNA repair, recombination, and replication. Annu Rev Biochem. 2014;83:519–52.
6. Ghosh A, Rossi ML, Aulds J, Croteau D, Bohr VA. Telomeric D-loops containing 8-oxo-2'-deoxyguanosine are preferred substrates for Werner and Bloom syndrome helicases and are bound by POT1. J Biol Chem. 2009;284:31074–84.
7. Poot M, Hoehn H, Runger TM, Martin GM. Impaired S-phase transit of Werner syndrome cells expressed in lymphoblastoid cell lines. Exp Cell Res. 1992;202:267–73.
8. Crabbe L, Verdun RE, Haggblom CI, Karlseder J. Defective telomere lagging strand synthesis in cells lacking WRN helicase activity. Science. 2004;306:1951–3.
9. Sidorova JM, Li N, Folch A, Monnat RJ Jr. The RecQ helicase WRN is required for normal replication fork progression after DNA damage or replication fork arrest. Cell Cycle. 2008;7:796–807.
10. Lebel M, Leder P. A deletion within the murine Werner syndrome helicase induces sensitivity to inhibitors of topoisomerase and loss of cellular proliferative capacity. Proc Natl Acad Sci USA. 1998;95:13097–102.
11. Constantinou A, Tarsounas M, Karow JK, Brosh RM, Bohr VA, Hickson ID, et al. Werner's syndrome protein (WRN) migrates Holliday junctions and co-localizes with RPA upon replication arrest. EMBO Rep. 2000;1:80–84.
12. Kusumoto R, Muftuoglu M, Bohr VA. The role of WRN in DNA repair is affected by post-translational modifications. Mech Ageing Dev. 2007;128:50–57.
13. Cheng WH, von Kobbe C, Opresko PL, Fields KM, Ren J, Kufe D, et al. Werner syndrome protein phosphorylation by Abl tyrosine kinase regulates its activity and distribution. Mol Cell Biol. 2003;23:6385–95.
14. Ammazzalorso F, Pirzio LM, Bignami M, Franchitto A, Pichierri P. ATR and ATM differently regulate WRN to prevent DSBs at stalled replication forks and promote replication fork recovery. EMBO J. 2010;29:3156–69.
15. Palermo V, Rinalducci S, Sanchez M, Grillini F, Sommers JA, Brosh RM Jr., et al. CDK1 phosphorylates WRN at collapsed replication forks. Nat Commun. 2016;7:12880.
16. Pichierri P, Rosselli F, Franchitto A. Werner's syndrome protein is phosphorylated in an ATR/ATM-dependent manner following replication arrest and DNA damage induced during the S phase of the cell cycle. Oncogene. 2003;22:1491–1500.
17. Yannone SM, Roy S, Chan DW, Murphy MB, Huang S, Campisi J, et al. Werner syndrome protein is regulated and phosphorylated by DNA-dependent protein kinase. J Biol Chem. 2001;276:38242–8.
18. Li K, Casta A, Wang R, Lozada E, Fan W, Kane S, et al. Regulation of WRN protein cellular localization and enzymatic activities by SIRT1-mediated deacetylation. J Biol Chem. 2008;283:7590–8.
19. Muftuoglu M, Kusumoto R, Speina E, Beck G, Cheng WH, Bohr VA. Acetylation regulates WRN catalytic activities and affects base excision DNA repair. PLoS ONE 2008;3:e1918.
20. Blander G, Zalle N, Daniely Y, Taplick J, Gray MD, Oren M. DNA damage-induced translocation of the Werner helicase is regulated by acetylation. J Biol Chem. 2002;277:50934–40.
21. Kawabe Y, Seki M, Seki T, Wang WS, Imamura O, Furuichi Y, et al. Covalent modification of the Werner's syndrome gene product with the ubiquitin-related protein, SUMO-1. J Biol Chem. 2000;275:20963–6.
22. Su F, Bhattacharya S, Abdisalaam S, Mukherjee S, Yajima H, Yang Y, et al. Replication stress induced site-specific phosphorylation targets WRN to the ubiquitin-proteasome pathway. Oncotarget. 2016;7:46–65.
23. Li K, Wang R, Lozada E, Fan W, Orren DK, Luo J. Acetylation of WRN protein regulates its stability by inhibiting ubiquitination. PLoS ONE 2010;5:e10341.
24. Shamanna RA, Lu H, Croteau DL, Arora A, Agarwal D, Ball G, et al. Camptothecin targets WRN protein: mechanism and relevance in clinical breast cancer. Oncotarget. 2016;7:13269–84.
25. Momand J, Zambetti GP, Olson DC, George D, Levine AJ. The mdm-2 oncogene product forms a complex with the p53 protein and inhibits p53-mediated transactivation. Cell. 1992;69:1237–45.
26. Honda R, Tanaka H, Yasuda H. Oncoprotein MDM2 is a ubiquitin ligase E3 for tumor suppressor p53. FEBS Lett. 1997;420:25–27.
27. Wu X, Bayle JH, Olson D, Levine AJ. The p53-mdm-2 autoregulatory feedback loop. Genes & Dev. 1993;7:1126–32.
28. Tollini LA, Jin A, Park J, Zhang Y. Regulation of p53 by Mdm2 E3 ligase function is dispensable in embryogenesis and development, but essential in response to DNA damage. Cancer Cell 2014;26:235–47.
29. Itahana K, Mao H, Jin A, Itahana Y, Clegg HV, Lindstrom MS, et al. Targeted inactivation of Mdm2 RING finger E3 ubiquitin ligase activity in the mouse reveals mechanistic insights into p53 regulation. Cancer Cell 2007;12:355–66.
30. Wade M, Li YC, Wahl GM. MDM2, MDMX and p53 in oncogenesis and cancer therapy. Nat Rev Cancer. 2013;13:83–96.
31. Toledo F, Wahl GM. Regulating the p53 pathway: in vitro hypotheses, in vivo veritas. Nat Rev Cancer. 2006;6:909–23.
32. Vousden KH, Lu X. Live or let die: the cell's response to p53. Nat Rev Cancer. 2002;2:594–604.
33. Shieh SY, Ikeda M, Taya Y, Prives C. DNA damage-induced phosphorylation of p53 alleviates inhibition by MDM2. Cell 1997;91:325–34.
34. Mikawa T, Maruyama T, Okamoto K, Nakagama H, Lleonart ME, Tsusaka T, et al. Senescence-inducing stress promotes proteolysis of phosphoglycerate mutase via ubiquitin ligase Mdm2. J Cell Biol. 2014;204:729–45.
35. Brenkman AB, de Keizer PL, van den Broek NJ, Jochemsen AG, Burgering BM. Mdm2 induces mono-ubiquitination of FOXO4. PLoS ONE 2008;3:e2819.
36. Uchida C, Miwa S, Kitagawa K, Hattori T, Isobe T, Otani S, et al. Enhanced Mdm2 activity inhibits pRB function via ubiquitin-dependent degradation. EMBO J. 2005;24:160–9.
37. Vassilev LT, Vu BT, Graves B, Carvajal D, Podlaski F, Filipovic Z, et al. In vivo activation of the p53 pathway by small-molecule antagonists of MDM2. Science. 2004;303:844–8.
38. Rufini A, Tucci P, Celardo I, Melino G. Senescence and aging: the critical roles of p53. Oncogene. 2013;32:5129–43.
39. Zuckerman V, Wolyniec K, Sionov RV, Haupt S, Haupt Y. Tumour suppression byp53: the importance of apoptosis and cellular senescence. J Pathol. 2009;219:3–15.
40. Wu ZH, Shi Y, Tibbetts RS, Miyamoto S. Molecular linkage between the kinase ATM and NF-kappaB signaling in response to genotoxic stimuli. Science. 2006;311:1141–6.
41. Kang C, Xu Q, Martin TD, Li MZ, Demaria M, Aron L, et al. The DNA damage response induces inflammation and senescence by inhibiting autophagy of GATA4. Science. 2015;349:aaa5612.